Andrea Kroner (Autor)

# VCSEL-Based Optical Trapping Systems for Microfluidic Applications

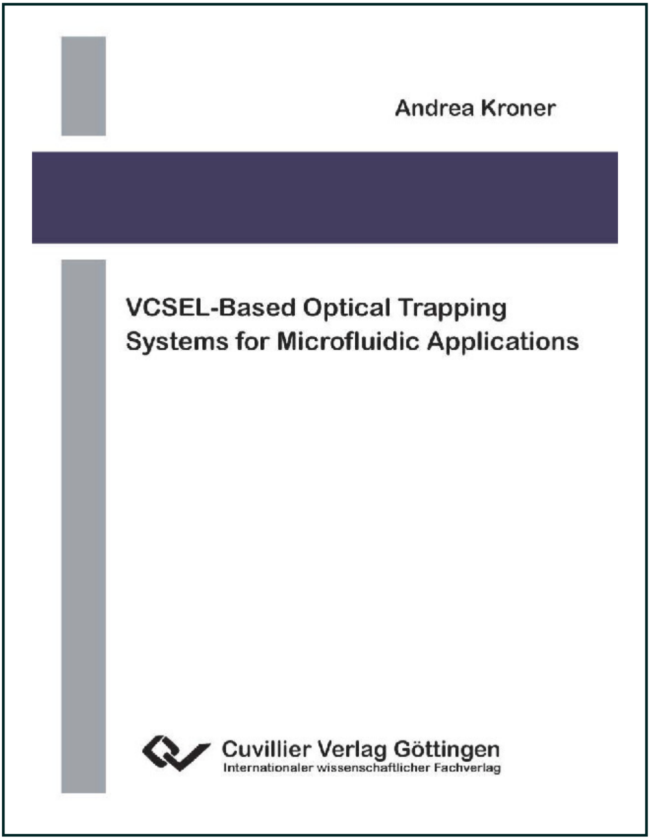


https://cuvillier.de/de/shop/publications/494

# 2 Optical Particle Manipulation and Trapping

Optical manipulation describes the exertion of force on matter by light. As early as four centuries ago this kind of light-matter interaction was observed by Johannes Kepler. He noticed that tails of comets always point away from the sun, which he attributes to a sort of radiation pressure [4]. However, it was not until the invention of the laser that this effect could be demonstrated in laboratories as well. In experiments, mesoscopic particles were not only moved and guided by light, but also fixed in space over a long period, hence the terms optical trap or optical tweezers are often used.

Since its first demonstration optical manipulation has gained increasing interest in various scientific fields. In atom physics laser trapping enabled atom cooling and the generation of Bose-Einstein condensates [13]. Furthermore, sophisticated optical tweezers systems can be used for force measurements on particles with sub-piconewton resolution [14]. In the field of biophotonics, the direct handling of single cells or DNA bound to microbeads [1] opened up new research opportunities like cell immobilization during spectral studies [2].

## 2.1 Theory of Optical Manipulation

### 2.1.1 Basic Working Principle

To estimate the maximum force that can be exerted on matter by radiation pressure, a ray of light hitting a totally reflecting mirror is assumed. When reflected straight back, the change in momentum of a single photon of this ray is

$$\Delta p_{\mathrm{ph}} = 2\frac{\hbar\omega}{c} = 2\frac{E_{\mathrm{ph}}}{c}, \tag{2.1}$$

where $c$ is the vacuum velocity of light, $\hbar$ is the reduced Planck constant, $\omega$ is the angular frequency and $E_{\mathrm{ph}} = \hbar\omega$ is the photon energy. Since the total momentum must be conserved, momentum is transferred from the photon to the mirror. Thus, the mirror experiences a total force of

$$F = N\frac{\Delta p_{\mathrm{ph}}}{\Delta t} = \frac{2}{c}\frac{NE_{\mathrm{ph}}}{\Delta t} = \frac{2}{c}P_{\mathrm{r}}, \tag{2.2}$$

with $N$ being the number of photons hitting the mirror during the time period $\Delta t$ and $P_{\mathrm{r}}$ being the optical power of the incident ray. For an optical power of 1 mW, this force is around 10 pN. Although this is too small to affect a macroscopic mirror, it could be enough to accelerate microscopic particles whose weight is in the same order of magnitude.

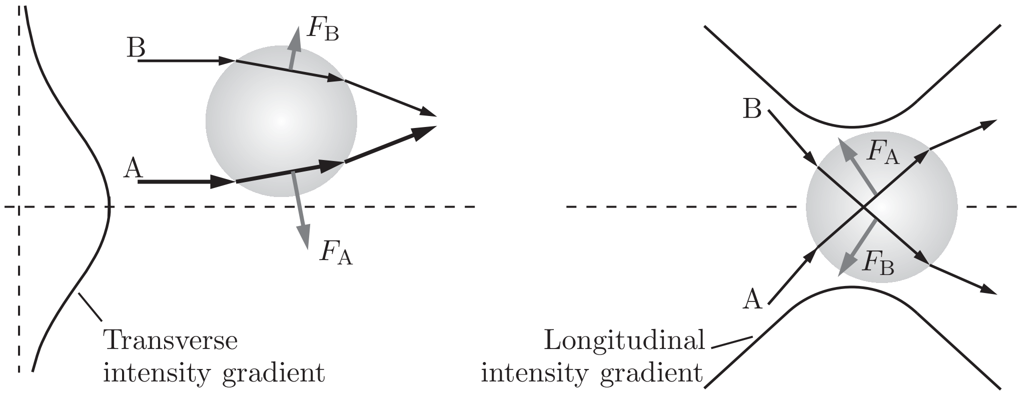


**Fig. 2.1:** Working principle of a two-dimensional optical trap (left). The refraction of a parallel laser beam with a transverse intensity gradient at a spherical, transparent particle leads to the forces $F_A$ and $F_B$. Since ray A is stronger than ray B, the net force points toward the intensity maximum. With a tightly focused laser beam (right) even three-dimensional trapping can be realized.

Based on this estimation, Arthur Ashkin performed an experiment on particle manipulation at Bell Laboratories, New Jersey in 1970 [15]. In former experiments, radiation forces were obscured by thermal forces, which arise due to temperature gradients in the illuminated particle and the surrounding medium [16]. Therefore, Ashkin used transparent, micrometer-sized latex spheres suspended in transparent water, so heating by absorption could be avoided. With a mildly focused laser beam of some milliwatts of optical power, particle motion in propagation direction with velocities of some μm/s was observed [13]. However, an additional force was found, which pulled particles from the fringe of the beam toward the center of the beam. Once there, they stayed stable on beam axis, while pushed forward by radiation pressure. The left hand side of Fig. 2.1 illustrates the occurrence of this unexpected force with a ray-optical model. Refraction of a ray at a particle surface is accompanied by a change in momentum of the corresponding photons as well. Thus, conservation of momentum demands a momentum transfer to the particle. For a parallel laser beam with a transverse intensity gradient, as shown in Fig. 2.1 (left), the rays A and B lead to the forces $F_A$ and $F_B$ on the particle. Caused by the offset between beam axis and particle center, ray A has higher power than ray B, so $F_A$ is larger than $F_B$. Therefore, the particle experiences a net force toward the intensity maximum, where it remains fixed in transverse direction. A two-dimensional or transverse optical trap is thus established. Since the net force in transverse direction arises from the intensity gradient, it is often termed gradient force, while the forward directed force, mainly caused by reflection at the particle surface, is commonly named scattering force.

For a focused laser beam, as shown on the right side of Fig. 2.1, also a longitudinal gradient force arises. If the beam is tightly focused and the corresponding intensity gradient is high, this force can overcome the scattering force. In this case, a three-dimensional optical trap, also called optical tweezers, is generated by a single laser beam. Here, the particle stays fixed near the focal point. Optical tweezers were demonstrated for the first time by Arthur Ashkin in 1986 [17], where different kinds of transparent particles with diameters of

10 μm down to 25 nm were stably trapped with optical power ranging from some milliwatts up to 1.4 W. In later experiments, trapping of biological matter like Escherichia coli (E. coli) bacteria and yeast cells was demonstrated, where even a reproduction of living cells during trapping could be observed [18]. It is important to note, that for stable trapping the gradient force must not only exceed the scattering force, but also any thermal motion of the particle [4, 17].

The way to describe trapping forces in more detail depends on the size of the trapped particle relative to the size of the incident wavelength. In the **Rayleigh regime**, where particles whose diameter $a$ is much smaller than the wavelength $\lambda$ are considered, a dielectric particle can be treated as a point dipole. The dipole moment of the particle, which is induced by the electrical field, scales with the polarizability $\alpha_\mathrm{p}$ of the dielectric material. In a spatially inhomogeneous electromagnetic field, a Lorentz force is exerted on the dipole, in order to minimize its energy in the intensity field [4, 19]. The gradient force acting on a spherical particle is given by [20]

$$\boldsymbol{F}_\mathrm{g} = \frac{2\pi}{\bar{n}_\mathrm{m}^2 c}\,\alpha_\mathrm{p}\,\nabla\mathcal{I} = \frac{\pi a^3}{4\,c}\left(\frac{m^2-1}{m^2+2}\right)\nabla\mathcal{I}, \tag{2.3}$$

where $m$ is the ratio of the refractive index of the particle $\bar{n}_\mathrm{p}$ to the index of the surrounding medium $\bar{n}_\mathrm{m}$, and $\mathcal{I}$ is the light intensity field. The gradient force is proportional to the polarizability of the particle and the strength of the intensity gradient. It is oriented along the gradient for $m > 1$ and reverse for $m < 1$, that is, particles with a lower refractive index than the surrounding medium are repelled by the beam. Additionally, Rayleigh scattering gives rise to a scattering force oriented along the propagation direction of the incident light. Without loss of generality, this is assumed to be in $z$-direction, so [20]

$$\boldsymbol{F}_\mathrm{s} = \frac{\bar{n}_\mathrm{m}\mathcal{I}}{c}\frac{\pi^5 a^6}{3\,\lambda^4}\left(\frac{m^2-1}{m^2+2}\right)^2\boldsymbol{e}_z. \tag{2.4}$$

The scattering force scales with the light intensity and increases for increasing contrast in refractive index $m = \bar{n}_\mathrm{p}/\bar{n}_\mathrm{m}$.

In the **Lorentz-Mie regime**, where the dimensions of particles are comparable to the wavelength of the trapping laser, the above given point-dipole approximation is no longer valid. Instead, a full electromagnetic theory is required, which gives consideration to diffraction issues and includes a description of light propagation and polarization at the focal point [4]. Although optical trapping and tweezing is most often used to handle particles in the Lorentz-Mie regime and experiments show no significant qualitative difference to behavior of Rayleigh particles, optical manipulation in the Lorentz-Mie regime is difficult to model.

A closed description of trapping forces can again be found for particles with dimensions much larger than the laser emission wavelength, the so-called **Mie regime** [4, 20]. Here, a ray-optical model can be used, as already done qualitatively in Fig. 2.1. For an accurate quantitative description of trapping forces it is however necessary to consider the Fresnel equations for reflection and refraction as well as multiple reflections inside the particle. Since most of the particles examined in the scope in this thesis have diameters in the range of about ten times the laser wavelength, this regime is discussed in more detail in the following section.

### 2.1.2 Description of Light Forces in a Ray-Optical Model

In the simple estimation of the radiation force on a totally reflecting mirror in Sect. 2.1.1, the considered ray was assumed to be reflected straight back. However, this is certainly not true for a ray hitting a spherical, transparent particle, due to the curved surface and the partly transmitted power. Therefore, only a certain fraction $Q_\mathrm{s}$ of the incident power of the ray $P_\mathrm{r}$ contributes to the forward scattering force [21]

$$F_\mathrm{sr} = \frac{\bar{n}_\mathrm{m} P_\mathrm{r}}{c} Q_\mathrm{s}, \tag{2.5}$$

where $\bar{n}_\mathrm{m}$ is the refractive index of the surrounding medium. Same holds true for the transverse gradient force

$$F_\mathrm{gr} = \frac{\bar{n}_\mathrm{m} P_\mathrm{r}}{c} Q_\mathrm{g}. \tag{2.6}$$

To calculate the scaling factors $Q_\mathrm{s}$ and $Q_\mathrm{g}$, Fig. 2.2 has to be considered. A single ray hits the particle surface under an angle $\theta_\mathrm{i}$ and splits into the reflected ray of power $P_\mathrm{r}\mathcal{R}$ and an infinite number of emergent refracted rays of decreasing powers $P_\mathrm{r}\mathcal{T}^2$, $P_\mathrm{r}\mathcal{T}^2\mathcal{R}$, $P_\mathrm{r}\mathcal{T}^2\mathcal{R}^2$, .... The quantities $\mathcal{R}$ and $\mathcal{T}$ are the Fresnel coefficient for reflection and transmission at the interface under the angle $\theta_\mathrm{i}$, respectively. By summing up the contributions to momentum transfer in forward and transverse direction in an infinite series, $Q_\mathrm{s}$ and $Q_\mathrm{g}$ can be determined as [22]

$$Q_\mathrm{s} = 1 + \mathcal{R}\cos(2\theta_\mathrm{i}) - \frac{\mathcal{T}^2\left[\cos(2\theta_\mathrm{i} - 2\theta_\mathrm{t}) + \mathcal{R}\cos(2\theta_\mathrm{i})\right]}{1 + \mathcal{R}^2 + 2\mathcal{R}\cos(2\theta_\mathrm{t})}, \tag{2.7}$$

and

$$Q_\mathrm{g} = -\mathcal{R}\sin(2\theta_\mathrm{i}) + \frac{\mathcal{T}^2\left[\sin(2\theta_\mathrm{i} - 2\theta_\mathrm{t}) + \mathcal{R}\sin(2\theta_\mathrm{i})\right]}{1 + \mathcal{R}^2 + 2\mathcal{R}\cos(2\theta_\mathrm{t})}, \tag{2.8}$$

where $\theta_\mathrm{t}$ is the angle of refraction. More details on the derivation and the following calculation of the trapping force can be found in App. D.

Figure 2.3 shows the magnitude of both scaling factors depending on the position of incidence of the ray on the particle, which can be described by the radial component $r$ and the angular component $\varphi$. A large radial component thus corresponds to a large angle of

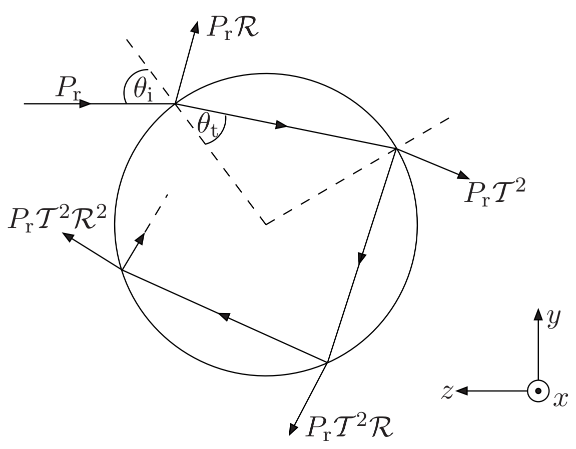


**Fig. 2.2:** Momentum transfer of a single ray of power $P_\mathrm{r}$ to a spherical particle: the ray hits the sphere under an angle $\theta_\mathrm{i}$ and splits into one reflected ray and an infinite number of refracted rays.

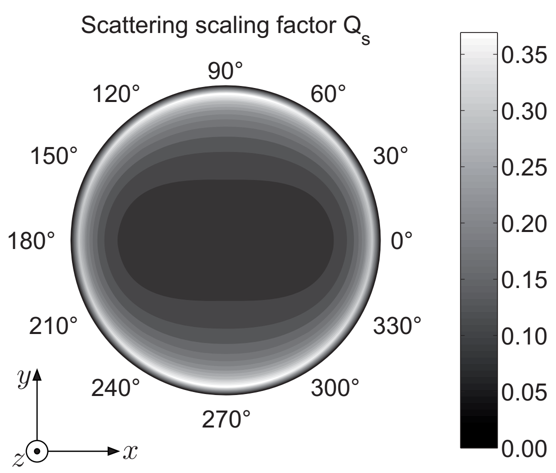


**Fig. 2.3:** Magnitude of the scaling factors for scattering ($Q_\mathrm{s}$, left) and gradient force ($Q_\mathrm{g}$, right) depending on the position of incidence of the ray on the particle.

incidence $\theta_\mathrm{i}$. The calculation is done for a polystyrene sphere ($\bar{n}_\mathrm{p} \approx 1.6$) in water ($\bar{n}_\mathrm{m} = 1.33$). The angular asymmetry arises from the dependence of the Fresnel coefficients on the polarization of the light, which is assumed to be linear and oriented in $x$-direction. Both scaling factors show high values close to the fringe of the particle. For the scattering component, this is due to the strong increase of the Fresnel reflection coefficient for large angles of incidence. The increase of the gradient component is caused by the strong deflection of the beam when refracted, corresponding to a high transfer of momentum. Accordingly, the gradient scaling factor decreases to zero for rays hitting the center of the particle, since the transmitted portion of the beam is not deflected. However, the reflected portion contributes completely to the scattering force, since the ray is reflected straight back. Thus, $Q_\mathrm{s}$ is slightly larger than zero at the particle center (not visible in the figure).

For the further calculation of the trapping force it is assumed that the particle is illuminated by a parallel laser beam with a transverse Gaussian power density distribution $S$. The beam axis is shifted by an offset of length $s$ to the particle center. Figure 2.4 shows a schematic side-view of the arrangement (left) as well as a projection of the power density distribution on the particle surface. The example is given for a sphere of $a = 6\,\mu\mathrm{m}$ diameter, a total optical power of $P = 5\,\mathrm{mW}$, a beam diameter of $2w_0 = 5\,\mu\mathrm{m}$ and an offset of $1\,\mu\mathrm{m}$ at $45\,^\circ$. Based on the determined scaling factors $Q_\mathrm{s}(r,\varphi)$ and $Q_\mathrm{g}(r,\varphi)$ and the given power density distribution $S(r,\varphi)$, the scattering and gradient force per area can be calculated according to (2.5) and (2.6) as

$$F_\mathrm{sa} = \frac{\bar{n}_\mathrm{m} S}{c} Q_\mathrm{s} \quad \text{and} \quad F_\mathrm{ga} = \frac{\bar{n}_\mathrm{m} S}{c} Q_\mathrm{g}. \tag{2.9}$$

The results are shown in Fig. 2.5 as a projection on the particle surface. The scattering force is especially strong at the upper right fringe of the sphere, thus, not only a forward movement of the particle is to be expected, but also a rotation. While the scattering force shows a clear contribution at the particle center, the gradient force decreases to zero and shows a donut like behavior. For better understanding, the direction of the gradient force is given by arrows in the graph. The force contributions in $135\,^\circ$ and $315\,^\circ$ direction are

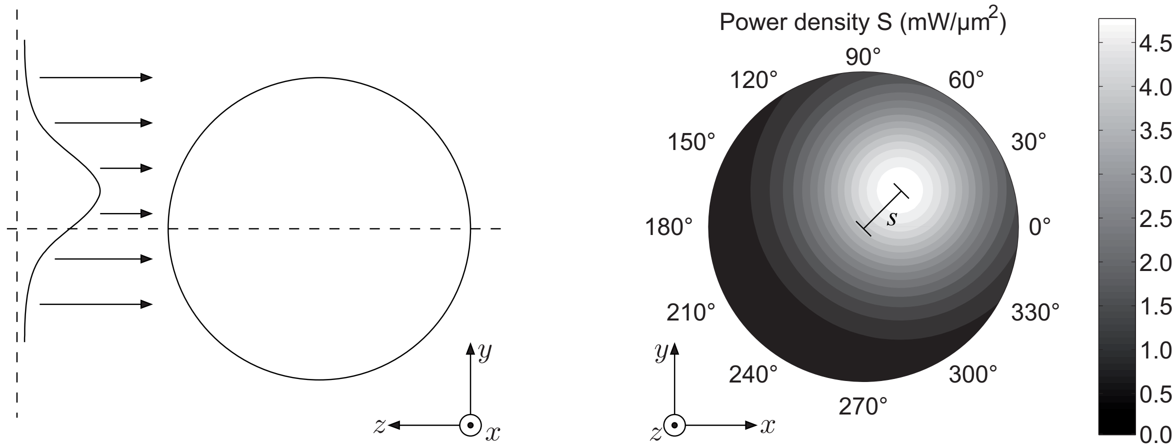


**Fig. 2.4:** Left: schematic side-view on the particle, which is illuminated by a parallel beam with transverse Gaussian power density distribution. Right: projection of the power density distribution on the particle, showing the offset $s$ between particle center and beam center.

approximately the same and cancel each other out, so no particle movement will occur in those directions. However, the force contribution in 45° direction is much stronger than the opposite one, so the particle will effectively be moved towards the maximum intensity of the parallel beam.

The total radiation force on the particle can be determined by integrating the force per area over the projected area of the particle. In case of the gradient force, this has to be done separately for the components in $x$- and $y$-direction, where $F_{\mathrm{ga}\,x} = F_{\mathrm{ga}} \cos\varphi$ and $F_{\mathrm{ga}\,y} = F_{\mathrm{ga}} \sin\varphi$

$$F_{\mathrm{s}} = \int_0^{2\pi} \int_0^{a/2} F_{\mathrm{sa}}(r,\varphi)\, r \mathrm{d}r\, \mathrm{d}\varphi, \tag{2.10}$$

$$F_{\mathrm{g}\,x,y} = \int_0^{2\pi} \int_0^{a/2} F_{\mathrm{ga}\,x,y}(r,\varphi)\, r \mathrm{d}r\, \mathrm{d}\varphi. \tag{2.11}$$

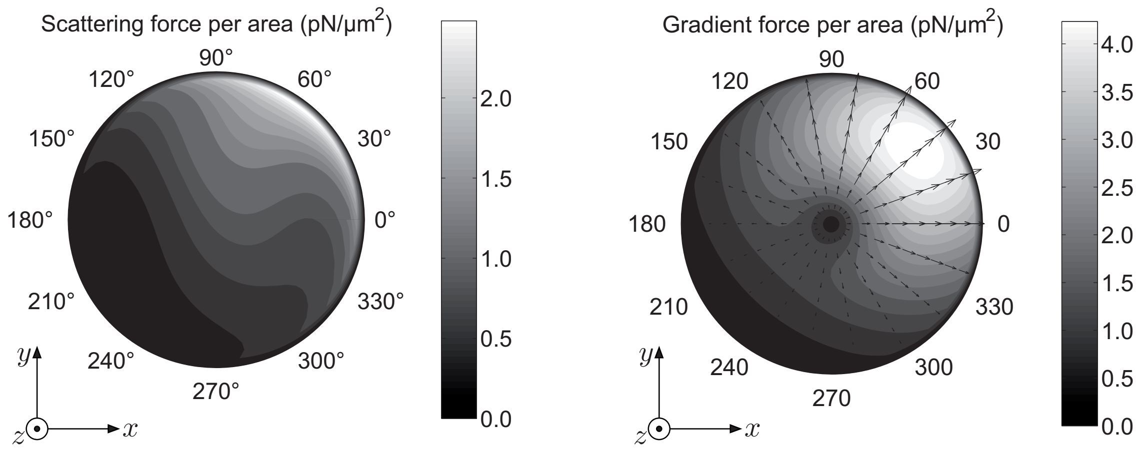


**Fig. 2.5:** Calculated scattering and gradient fore per area as a projection on the particle surface.